Title

Lin28a Regulates Pathological Cardiac Hypertrophic Growth Through Pck2-Mediated Enhancement of Anabolic Synthesis.

Journal

Circulation, 139(14)

Authors

Ma, Hong

Yu, Shuo

Liu, Xiaojing

et al.

Publication Date

2019-04-02

DOI

10.1161/CIRCULATIONAHA.118.037803

Peer reviewed

HHS Public Access

Author manuscript

Circulation. Author manuscript; available in PMC 2020 April 02.

Published in final edited form as:

Circulation. 2019 April 02; 139(14): 1725–1740. doi:10.1161/CIRCULATIONAHA.118.037803.

Lin28a Regulates Pathological Cardiac Hypertrophic Growth through Pck2-mediated Enhancement of Anabolic Synthesis

Hong Ma, MD, PhD[1,2], **Shuo Yu, MD**[1,2], **Xiaojing Liu, PhD**[3], **Yingao Zhang, BS**[1,2], **Thomas Fakadej, BS**[1,2], **Ziqing Liu, PhD**[1,2], **Chaoying Yin, PhD**[1,2], **Weining Shen, PhD**[4], **Jason W. Locasale, PhD**[3], **Joan M. Taylor, PhD**[1,2], **Li Qian, PhD**[1,2], and **Jiandong Liu, PhD**[1,2]

[1]Department of Pathology and Laboratory Medicine, University of North Carolina at Chapel Hill, Chapel Hill, NC 27599, USA.

[2]McAllister Heart Institute, University of North Carolina at Chapel Hill, Chapel Hill, NC 27599, USA.

[3]Department of Pharmacology and Cancer Biology, Duke University School of Medicine, Duke University, Durham, NC 27710, USA.

[4]Department of Statistics, University of California at Irvine, Irvine, CA 92697, USA.

Abstract

BACKGROUND: Hypertrophic response to pathological stimuli is a complex biological process that involves transcriptional and epigenetic regulation of the cardiac transcriptome. Though previous studies have implicated transcriptional factors and signaling molecules in pathological hypertrophy, the role of RNA-binding protein (RBP) in this process has received little attention.

METHODS: Here we used transverse aortic constriction (TAC) and *in vitro* cardiac hypertrophy models to characterize the role of an evolutionary conserved RBP Lin28a in pathological cardiac hypertrophy. Next generation sequencing, RNA immunoprecipitation and gene expression analyses were applied to identify the downstream targets of Lin28a. Epistatic analysis, metabolic assays and flux analysis were further utilized to characterize the effects of Lin28a and its downstream mediator in cardiomyocyte hypertrophic growth and metabolic remodeling.

RESULTS: Cardiac-specific deletion of *Lin28a* attenuated pressure overload-induced hypertrophic growth, cardiac dysfunction and alterations in cardiac transcriptome. Mechanistically, Lin28a directly bound to mitochondrial phosphoenolpyruvate carboxykinase 2 (*Pck2*) mRNA and increased its transcript level. Increasing *Pck2* was sufficient to promote hypertrophic growth similar to that caused by increasing Lin28a, whereas knocking down *Pck2* attenuated norepinephrine-induced cardiac hypertrophy. Epistatic analysis demonstrated that Pck2 mediated, at least in part, the role of Lin28a in cardiac hypertrophic growth. Furthermore,

Correspondence: Li Qian, PhD, or Jiandong Liu, PhD, Department of Pathology and Laboratory Medicine, McAllister Heart Institute, University of North Carolina at Chapel Hill, 111 Mason Farm Road, Chapel Hill, NC 27599, USA. Phone: 919-962-0340 (L.Q.) or 919-962-0326 (J.L.). Fax: 919-966-6718. li_qian@med.unc.edu or jiandong_liu@med.unc.edu.

Disclosures

None.

metabolomic analyses highlighted role for Lin28a and Pck2 in promoting cardiac biosynthesis required for cell growth.

CONCLUSIONS: Our study demonstrates that Lin28a promotes pathological cardiac hypertrophy and glycolytic reprograming, at least in part by binding to and stabilizing *Pck2* mRNA.

Keywords

Pathological cardiac hypertrophy; Pressure overload; Lin28a; Pck2; Biosynthesis; Glycolysis; Metabolism

INTRODUCTION

Cardiac hypertrophy is often associated with diverse pathological conditions such as mechanical overload, hypertension and ischemic injury.[1, 2] While the hypertrophic mechanism has been generally regarded as compensatory in conferring resistance to cardiac stress, prolonged growth predisposes individuals to intractable heart failure and sudden cardiac death. As such, recent basic and preclinical studies suggest that attenuation of pathological hypertrophy has a beneficial effect of mitigating the development of heart failure,[1, 3] making it a promising target for therapeutic interventions. While significant advances in treatment of pathological hypertrophy has been achieved, the commonly prescribed medications for pathological hypertrophy, including angiotensin-converting enzyme inhibitors, angiotensin receptor blockers, beta-receptor blockers, calcium channel blockers and others, usually bring about regression of left ventricular mass by 10 ~ 20% in human patients,[4] an in-depth knowledge of the molecular basis of this detrimental process could have considerable impact for the development of more potent therapeutics.[4, 5]

When subjected to pathological stimuli, the heart undergoes extensive metabolic and structural changes characterized by a switch from fatty acid oxidation to greater reliance on glycolysis and hypertrophic growth of the cardiomyocytes, respectively.[6] The hypertrophic heart also demonstrates enhanced flux of metabolic intermediates into biosynthesis. Although the effect of metabolic remodeling on cell growth and/or proliferation has been increasingly recognized, questions remain on whether and how the metabolic remodeling during pathological hypertrophy contributes to myocardial hypertrophic growth, as well as the molecular regulation of this metabolic remodeling.

The extensive cardiac structural and metabolic changes during pathological hypertrophy involves profound global alterations in cardiac transcriptome.[7] In addition to transcriptional regulation of cardiac gene expression,[8] RNA-binding proteins (RBPs)-mediated posttranscriptional regulation has emerged as a critical layer for control of gene function during health and diseases.[9, 10] The RBPs bind to diverse RNAs and intimately influence every aspect of RNAs' metabolism throughout their lifecycle, including biogenesis, stability, splicing, cellular localization, and translation.[10, 11] Through inhibition of microRNA *let-7* maturation and/or directly binding to mRNAs to regulate their abundance and translation, the evolutionarily conserved RBP Lin28a and its paralogue Lin28b play critical roles in pluripotency, organismal growth, tissue repair and oncogenesis.[12, 13] Much of these diverse

functions of Lin28 has been attributed to its role in regulating cellular metabolism, yet the exact mechanisms differ depending on the biological contexts, highlighting the complexity of Lin28-mediated metabolic regulation. For instance, in the context of whole-animal physiology, Lin28 modulates glucose metabolism through regulating mTOR signaling in a *let-7*-dependent manner.[14] In contrast, during tissue repair, Lin28 enhances glycolysis and oxidative phosphorylation (OxPhos) independently of *let-7* by directly binding to and enhancing the translation of the mRNAs of multiple rate-limiting enzymes involved in the glycolysis and OxPhos.[15] A recent study on oncogenesis further demonstrates an important role of Lin28 in promoting aerobic glycolysis in cancer cells via targeting pyruvate dehydrogenase kinase 1.[16] Despite the important role of Lin28 in metabolic regulation, it remains to be explored whether Lin28 may regulate cardiac metabolism during pathological hypertrophy, and how exactly this regulation contributes to pathological structural remodeling.

In this study, we revealed a critical role of Lin28a in pathological cardiac hypertrophy and metabolic re-patterning. Cardiac-specific deletion of *Lin28a* blunted pressure overload-induced cardiac hypertrophy and suppressed cardiac fibrosis. This effect of *Lin28a* on cardiac pathological hypertrophy likely occurred in a *let-7*-independent manner. Through RNA deep-sequencing, bioinformatics analyses and RNA immunoprecipitation assay, we identified *Pck2*, which encodes the mitochondrial phosphoenolpyruvate carboxykinase, as a direct target of Lin28a in cardiomyocytes. Lin28a directly bound to *Pck2* mRNA, and positively impacted its expression level. Remarkably, whereas knockdown of *Pck2* partially suppressed Lin28a-induced cardiomyocyte hypertrophic growth, overexpressing *Pck2* reversed the attenuation of norepinephrine-induced hypertrophy by loss of *Lin28a* function. Furthermore, metabolomic analyses indicated that Lin28a/Pck2 axis promoted cardiac biosynthesis required for cell growth. Our study thus demonstrates that Lin28a promotes pathological cardiac hypertrophy through regulating biosynthesis.

METHODS

The data, analytic methods, and study materials will be made available to other researchers for purposes of reproducing the results or replicating the procedure on reasonable request. The detailed methods are provided in the online-only Data Supplement.

Animals

All experiments involving animals were performed in accordance with the University of North Carolina at Chapel Hill Institutional Animal Care and Use Committee (IACUC) approved protocols.

Statistical Analysis

All data were presented as mean ± SEM and statistically analyzed using SPSS or Prism software. Two-tailed independent sample t test was used to compare the mean difference between two groups. One-way or two-way ANOVA was used to compare the mean from three or more groups. If ANOVA analysis showed significant difference, then the Least Significant Difference (LSD) test or the Tukey's multiple comparison test was applied for

post hoc analysis to detect the pairwise difference while adjusting for multiplicity. $P < 0.05$ was considered statistically significant.

RESULTS

Upregulation of *Lin28a* by Mechanical and Neurohumoral Stimuli

Previous studies demonstrated that *Lin28a* responds to cellular stress[17] and promotes tissue repair[15], we thus postulate that *Lin28a* may play a role in cardiac remodeling under stress condition. To test this hypothesis, we first determined if *Lin28a* responded to mechanical stress. We analyzed *Lin28a* expression in a mouse model of cardiac hypertrophy whereby the transverse aorta was constricted to induce pressure overload. Unlike its paralogue *Lin28b, Lin28a* was barely detectable in sham-operated control mouse hearts, yet, its expression was rapidly induced at both transcript and protein levels in the adult hearts following transverse aortic constriction (TAC) with the protein expression reaching its peak level at 3 days after TAC surgery (Figure 1A and1B, Supplemental Figure 1A and 1B, and Supplemental Table 1). We also found that the response of *Lin28a* to TAC surgery was similar, albeit slightly delayed, to that of the early response genes such as *c-Jun* and *c-Myc* (Supplemental Figure 1A and Supplemental Table 1), suggesting that Lin28a might act downstream of the early response genes.[18, 19] In parallel, we assessed the response of *Lin28a* expression to neurohormonal agonists. Likewise, *Lin28a*, but not *Lin28b*, was significantly upregulated in isolated neonatal rat cardiomyocytes (NRCMs) in response to angiotensin II or norepinephrine (NE) (Figure 1C).

Lin28a Plays a Significant Role in NE-induced Cardiac Hypertrophy

As a first step to test the requirement for *Lin28a* in stress-induced cardiac hypertrophy, we assessed the effect of manipulating *Lin28* expression on NE-induced NRCM hypertrophy. Whereas NRCMs infected with non-targeting siRNA control (si*NT*) developed massive hypertrophy after *NE* treatment, the NE-induced NRCMs enlargement was markedly suppressed by siRNAs against *Lin28a* (si*Lin28a*) (Figure 1D–1F and Supplemental Figure 1C). Consistently, si*Lin28a* suppressed NE-induced upregulation of hypertrophic markers atrial natriuretic peptide (*Anp*) and brain natriuretic peptide (*Bnp*) (Figure 1G and1H). Conversely, lentiviral-mediated *Lin28a* overexpression (Lenti-*Lin28a*) caused a substantial increase in the size of NRCMs compared to lentiviral control (Lenti-*Con*) (Figure 1I and1J and Supplemental Figure 1D), and upregulated the expression of *Anp* and *Bnp* (Figure 1K and1L). More importantly, lentiviral-mediated *Lin28a* overexpression in adult mouse hearts also upregulated the expression of fetal genes such as *Anp*, *Bnp*, α-skeletal muscle actin (*Acta1*), and myosin heavy chain beta (*Myh7*), and led to an increase in cardiomyocyte size (Supplemental Figure 1E–1G and Supplemental Table 1, and data not shown).

Loss of Cardiac *Lin28a* Blunted Pressure Overload-induced Cardiac Hypertrophy

Next, we sought to determine the functional involvement of *Lin28a* in stress-induced cardiac hypertrophy *in vivo*. Cardiac-specific *Lin28a* knockout model ($Lin28a^{Cko}$) was generated by crossing $Lin28a^{fl/fl}$ mice with *Mlc2v-Cre* mice. Western blot analysis indicated that Cre-mediated conditional knockout of *Lin28a* reduced Lin28a protein level by at least 70% (Supplemental Figure 2A). The $Lin28a^{Cko}$ mice and control $Lin28a^{fl/fl}$ mice were then

subjected to sham or TAC surgery. In the sham group, the gross morphology of *Lin28a*^{Cko} hearts did not differ from that of *Lin28a*$^{fl/fl}$ hearts (Figure 2A). Additionally, we did not observe significant differences in the heart to body weight ratio (HW/BW) between *Lin28a*^{Cko} mice and *Lin28a*$^{fl/fl}$ mice (5.40±0.06 vs 5.34 ±0.15 mg/g, P>0.05; Figure 2B). In contrast, TAC induced a significant increase in the size of *Lin28a*$^{fl/fl}$ hearts, and this TAC-induced hypertrophic growth was substantially suppressed by cardiac ablation of *Lin28a* (Figure 2A). Consistently, *Lin28a*^{Cko} mice demonstrated substantially decreased HW/BW compared to the *Lin28a*$^{fl/fl}$ mice following TAC surgery (7.84±0.29 vs 9.86±0.48 mg/g, P<0.05; Figure 2B). To further evaluate the effect of cardiac specific *Lin28a* ablation on TAC-induced cardiac hypertrophy, we measured myocardial wall thickness of *Lin28a*^{Cko} and *Lin28a*$^{fl/fl}$ hearts at end diastole (Figure 2C). At baseline, the thickness of *Lin28a*^{Cko} myocardial wall, including both left ventricular posterior wall (LVPWd) and interventricular septum (IVSd), was comparable to that of their control *Lin28a*$^{fl/fl}$ littermates (LVPWd: 0.79±0.03 vs 0.78±0.02 mm, P>0.05; IVSd: 0.78±0.03 vs 0.76±0.02 mm, P>0.05. Figure 2D and2E). While both dimensions were substantially increased in *Lin28a*$^{fl/fl}$ hearts by TAC at 1 week post-surgery, *Lin28a*^{Cko} hearts exhibited only mild increase in left ventricular wall thickness in response to TAC. Two and four weeks after TAC, the difference in the myocardial wall thickness between the two genotypes was even greater. For instance, at 4 weeks after TAC, LVPWd and IVSd increased by 90.2% and 91.5%, respectively, in *Lin28a*$^{fl/fl}$ mice relative to baseline, whereas these dimensions increased only by 28.5% and 30.1%, respectively in *Lin28a*^{Cko} mice (Figure 2D and2E).

At the cellular level, pathological cardiac hypertrophy is characterized by an increase in cardiomyocyte size. To determine if the attenuation of hypertrophy by loss of *Lin28a* function was attributable to alteration in cardiomyocyte size, we labeled cardiomyocytes with WGA and α-Actinin double immunostaining (Figure 2F). No significant difference was found in cardiomyocyte size between sham-operated *Lin28a*^{Cko} and *Lin28a*$^{fl/fl}$ hearts (220.30±8.75 vs 218.57±4.62, P>0.05; Figure 2F). However, cardiac ablation of *Lin28a* significantly suppressed TAC-induced enlargement of myocyte size (229.32±6.84 vs 328.14±8.92, P<0.01; Figure 2F).

We examined the effect of *Lin28a* ablation on cardiac hypertrophic marker genes expression. The upregulation of the fetal genes, including *Anp*, *Bnp*, and *Myh7*, observed in the hypertrophic hearts of *Lin28a*$^{fl/fl}$ mice was significantly suppressed in TAC-operated *Lin28a*^{Cko} hearts (Figure 2G). We also determined the expression of genes involved in cardiac function. The expression levels of ryanodine receptor 2 (*Ryr2*) and ATPase sarcoplasmic/endoplasmic reticulum Ca^{2+} transporting 2 (*Serca2*) were well preserved in TAC-operated *Lin28a*^{Cko} but not in *Lin28a*$^{fl/fl}$ hearts subjected to TAC (Figure 2H and Supplemental Figure 2B). Similar alterations in the expression seems to hold true also for several other genes important for cardiac contractility or function, such as Phospholamban (*Pln*), ATP synthase, and myosin light chain (*Myl*) (Supplemental Figure 2C), suggesting a potential beneficial effect of cardiac *Lin28a* ablation under pressure overload. Together, our studies demonstrate that *Lin28a* plays a critical role in both pressure overload and agonist-induced cardiac hypertrophy.

Loss of Cardiac *Lin28a* Attenuated Pressure Overload-induced Cardiac Remodeling

Cardiac fibrosis is a maladaptive response to pressure overload and contributes to the transition from hypertrophy towards intractable heart failure.[20, 21] We performed Picrosirius red staining to assess interstitial and perivascular fibrosis at 4 weeks after TAC. Under basal condition, neither *Lin28a*$^{fl/fl}$ nor *Lin28a*^{Cko} mice showed any sign of cardiac fibrosis (0.68±0.14% vs 0.75±0.15%, P>0.05; Figure 3A). Notably, TAC significantly increased fibrosis in interstitial and perivascular areas in *Lin28a*$^{fl/fl}$ hearts but not in *Lin28a*^{Cko} hearts (Figure 3A). This observation was further confirmed by analysis of collagen content with polarized light, which revealed collagen type I in yellow (Figure 3B).

Transforming growth factor β (TGF-β) signaling constitutes one of the most important signaling pathways required for cardiac fibrosis.[22, 23] TGF-β signaling induces activation of cardiac fibroblast and subsequent fibrogenesis partly through its downstream mediator connective tissue growth factor (*Ctgf*).[24, 25] Interestingly, gene expression analysis revealed that TAC-induced upregulation of TGF-β signaling components and *Ctgf* was suppressed by loss of *Lin28a* (Supplemental Figure 2D), suggesting that reduced activation of TGF-β signaling may underlie the decreased fibrosis in the *Lin28a*^{Cko} hearts after TAC. We then examined the expression of genes more directly involved in fibrosis. Collagen type I α1 (*Col1a1*) and collagen type III α1 (*Col3a1*) encode the major collagen types in cardiac fibrotic tissue. Consistent with Picrosirius red staining, we observed a significant upregulation of both *Col1a1* and *Col3a1* at 4 weeks after TAC, and this upregulation was attenuated in *Lin28a*^{Cko} hearts (Figure 3C and3D, Supplemental Figure 2D and Supplemental Table 1). Collagen turnover and homeostasis in the heart is also affected by the levels of matrix metalloproteinases (MMPs) and tissue inhibitors of metalloproteinase (TIMPs). Although the expression levels of matrix metallopeptidase 2 (*Mmp2*) and matrix metallopeptidase 9 (*Mmp9*) remained comparable between TAC-operated *Lin28a*^{Cko} and *Lin28a*$^{fl/fl}$ hearts (Figure 3E and3F), the expression of tissue inhibitor of metalloproteinase 1 (*Timp1*) and *Timp2* was significantly higher in *Lin28a*$^{fl/fl}$ control hearts compared to *Lin28a*^{Cko} hearts after TAC (Figure 3G, Supplemental Figure 2D and Supplemental Table 1). Our findings thus suggest a decrease in the synthesis and an increase in the degradation of collagen may contribute to the reduction in fibrosis observed in *Lin28a*^{Cko} hearts subjected to TAC.

Cardiac hypertrophy is a major risk factor for the development of heart failure, eventually leading to ventricular dilation and dysfunction.[1, 3] We performed echocardiographic measurement to assess long-term cardiac structural remodeling and function. At baseline, both *Lin28a*^{Cko} and *Lin28a*$^{fl/fl}$ mice showed comparable left ventricle diastolic dimension (LVIDd, 3.36±0.09 vs 3.27±0.18 mm, P>0.05; Figure 3H) and normal cardiac function (ejection fraction (EF), 83.01±1.54 vs 79.10±2.48, P>0.05; Figure 3I). In line with blunted hypertrophic growth, structural remodeling as indicated by LVID was alleviated in *Lin28a*^{Cko} hearts compared to *Lin28a*$^{fl/fl}$ hearts following TAC (Figure 3J–3L). Concomitantly, the TAC-operated *Lin28a*^{Cko} hearts exhibited reduced left ventricular end-diastolic volume (Figure 3M) and end-systolic volume (Figure 3N). More importantly, *Lin28a*^{Cko} mice displayed preservation of ventricular systolic function as evidenced by their significantly reduced decline in EF and fraction shorting (FS) (Figure 3O and3P).

Consistently, the survival rate of the *Lin28a*^{Cko} mice was improved (Figure 3Q). The improvement of cardiac performance may result from a combination of increased contractility and decreased fibrotic remodeling (Figure 3A–3D and Supplemental Figure 2C and 2D). Together, loss of *Lin28a* ameliorates pressure overload-induced cardiac dysfunction and improved long-term survival.

Cardiac Ablation of *Lin28a* Mitigated Pressure Overload-induced Alterations in Cardiac Transcriptomes

Given the well-known function of Lin28a in blocking *let-7* biogenesis,[26, 27] we determined if *let-7* miRNAs participated in Lin28a-mediated cardiac hypertrophy. Consistent with a prior report,[28] several members of the *let-7* family were found to be upregulated in control hearts subjected to TAC surgery (Supplemental Figure 3A–3C). However, cardiac-specific ablation of *Lin28a* did not further increase the expression of these *let-7* miRNAs. Additionally, comparison of *Lin28a* and *let-7* expression revealed that they were both upregulated after TAC during a similar time window (Supplemental Figure 3A–3C, see also Figure 1A and 1B), suggesting that the effect of Lin28a on cardiac hypertrophy is unlikely to be mediated by *let-7*. In addition to the established role in inhibiting *let-7* biogenesis, Lin28a also directly binds to mRNAs to enhance mRNA stability and/or translation efficiency.[17, 29–31] To identify potential *let-7* independent mechanisms underlying *Lin28a*-mediated cardiac hypertrophy, we conducted whole-genome wide RNA deep sequencing to profile the transcriptomes of *Lin28a*^{Cko} and control hearts at 5 days after sham or TAC, a time point shortly after Lin28a exhibited peak level of upregulation in response to TAC (Figure 1B). Boxplot, MA plots and clustering of the RNA-Sequencing data confirmed the consistency between the biological repeats for each condition (Supplemental Figure 4A–4D). Although the cardiac transcriptomes of *Lin28a*^{Cko} and *Lin28a*$^{fl/fl}$ mice were similar (Supplemental Figure 4E) and clustered closely together under baseline (Supplemental Figure 4C–4D), unsupervised hierarchical clustering (HC) analysis indicated that TAC markedly altered cardiac transcriptome of *Lin28a*$^{fl/fl}$ mice (Supplemental Figure 4C–4D, and Supplemental Figure 5A). The cardiac transcriptome of TAC-operated *Lin28a*^{Cko} mice, however, more closely resembled that of sham-operated controls than that of TAC-operated *Lin28a*$^{fl/fl}$ mice, suggesting that the effect of mechanical stress on cardiac transcriptome was mitigated by loss of *Lin28a* function (Supplemental Figure 4C–4D, and Supplemental Figure 5A).

We identified a total of 4706 genes differentially expressed between TAC-operated *Lin28a*^{Cko} and *Lin28a*$^{fl/fl}$ cardiac samples (Supplemental Figure 5B). Functional annotation of these differentially expressed genes using DAVID tools revealed that several previously reported pathways, such as metabolic, PI3K-Akt and MAPK signaling pathways were affected by loss of *Lin28a* function (Figure 4A). Notably, a close exploration of the differentially expressed metabolic gene sets using DAVID, pathway analysis (IPA), and gene set enrichment analysis (GSEA) demonstrated extensive alterations in multiple metabolic processes, including fatty acid oxidation, TCA cycle, oxidative phosphorylation, glycolysis, and pentose phosphate pathways (Figure 4B–4E, Supplemental Figure 5C–5D and Supplemental Figure 6), suggesting that loss of *Lin28a* function had a profound effect on cardiac metabolism during hypertrophy. In particular, both GSEA and IPA analyses indicated that TAC-induced downregulation of oxidative phosphorylation was alleviated by

cardiac ablation of *Lin28a* (Figure 4C–4E, and Supplemental Figure 6). For instance, detailed gene expression analysis demonstrated that TAC-operated *Lin28a*^{Cko} hearts showed significant higher expression of the genes encoding mitochondrial oxidation complex, such as Succinate Dehydrogenase (*Sdh*), NADH:Ubiquinone Oxidoreductase (*Nduf*), Cytochrome C Oxidase (*Cox*) and Ubiquinol-Cytochrome C Reductase (*Uqcr*) compared to *Lin28a*$^{fl/fl}$ hearts subjected to TAC (Supplemental Figure 2E), which may contribute to the improvement of cardiac function observed in *Lin28a*^{Cko} hearts subjected to TAC. Consistently, qRT-PCR analysis revealed a similar trend of metabolic gene expression changes between control NRCMs, NRCMs treated with NE, and NRCMs treated with NE and si*Lina28a* (Figure 4F).

Identification of Pck2 as a Direct Target of Lin28a

To gain insight into how Lin28a regulates pathological hypertrophic growth, we sought to identify direct targets of Lin28a among the differentially expressed genes that responded to loss of *Lin28a* function after TAC. Interestingly, several genome-wide studies have attempted to identify direct targets of Lin28a. We re-analyzed the CLIP-sequencing data generated by Cho J et al,[32] and found that 1249 genes were significantly enriched in Lin28a pull-down components. These 1249 genes were potentially direct targets of Lin28a as their mRNAs were directly bound to Lin28a protein. Among the differentially expressed genes in our RNA-seq data (total 4706 genes), and potential Lin28a direct targets (total 1249 genes), 47 and 19 of which were involved in the most enriched metabolic and PI3K-AKT pathways (Figure 5A). We focused on the overlapping candidate genes (Figure 5A) and performed qRT-PCR to further assess their expression in response to pathological hypertrophic stimuli. 15 out of these candidate genes showed a similar response to mechanical overload *in vivo* and neurohumoral stimuli *in vitro* (Figure 5B). We performed RNA immunoprecipitation assay to test whether these candidates were directly bound by Lin28a in cardiomyocytes. FLAG-tagged Lin28a was overexpressed in cardiomyocytes and was pulled down by anti-FLAG antibody (Figure 5C). qPCR analysis was then performed to determine the level of transcripts in the protein-RNA complex pulled-down by anti-FLAG antibody compared to that by anti-IgG controls (Figure 5D). *Pck2* was the most enriched candidate transcripts in the anti-FLAG fraction (Figure 5D, Supplemental Figure 7A, Supplemental Table 1 and Supplemental Table 2). To further examine the physical interaction between Lin28a and *Pck2* mRNA, lentiviruses expressing FLAG-tagged *Lin28a* were transduced into adult mouse hearts via myocardial injection. RNA immunoprecipitation demonstrated that *Pck2* mRNA was enriched in the anti-FLAG pull-down fraction (Supplemental Figure 7B). Through these selection criteria, we were able to narrow down to *Pck2* as the most prominent downstream target of Lin28a in cardiomyocytes (Figure 5D). To validate this finding, we performed qPCR analysis with RNA samples from the TAC-operated *Lin28a*$^{fl/fl}$ hearts, and found that these hearts exhibited a significantly upregulated *Pck2* level compared to sham-operated *Lin28a*$^{fl/fl}$ hearts (Figure 5E). Cardiac-specific knockout of *Lin28a* mitigated this TAC-induced upregulation of *Pck2* (Figure 5E). Likewise, *Pck2* expression was markedly upregulated in NE-treated hypertrophic NRCMs (Figure 5F). Furthermore, overexpression of *Lin28a* in NRCMs resulted in a remarkable increase in *Pck2* expression at both transcript and protein levels, whereas silencing of *Lin28a* downregulated *Pck2* expression by 46% in NRCMs (Figure 5G and5H, and Supplemental Figure 7C). These data

collectively demonstrate that *Pck2* mRNA is physically bound by Lin28a and its level is controlled by Lin28a during cardiac hypertrophy.

Genetic Interaction of *Lin28a* and *Pck2* in NE-induced Cardiac Hypertrophy

We sought to determine whether there existed a Lin28a/Pck2 axis in regulating cardiac hypertrophic growth. First, we examined the response of Pck2 to TAC surgery and found that Pck2 exhibited transient upregulation similar to that of Lin28a with its peak level of expression occurring at 5~7 days after TAC (Supplemental Figure 7D and 7E, see also Figure 1A and 1B). Then, we addressed the requirement for *Pck2* in NE-induced NRCMs hypertrophy. Analysis of NRCMs size demonstrated that knocking down *Pck2* resulted in attenuation of NE-induced increase in NRCMs size and upregulation of *Anp*, *Bnp*, *Acta1* and *Myh7* (Figure 5I–5L, and Supplemental Figure 7F–7H), indicating that Pck2 is required for the development of NE-induced cardiac hypertrophy. Conversely, overexpression of *Pck2* by transducing NRCMs with lentiviruses expressing *Pck2* (Lenti-*Pck2*) resulted in a similar, albeit less pronounced, NRCMs hypertrophic growth phenotype to that of overexpressing *Lin28a* (Figure 5M–5P and Supplemental Figure 7I–7K), and reactivated fetal gene expression indicated by the upregulation of *Anp*, *Bnp*, *Myh7* and *Acta1* (Figure 5O and5P, and Supplemental Figure 7J and 7K). Likewise, lentiviral-mediated *Pck2* overexpression in adult mouse hearts also led to enlargement of cardiomyocyte size and reactivation of fetal gene expression (Supplemental Figure 8A–8F). Since knockdown of *Lin*28a and overexpression of *Pck2* resulted in opposite phenotypes, we asked if overexpressing *Pck2* could reverse the attenuation of NE-induced NRCMs hypertrophy by loss of *Lin28a* function. To this end, we introduced the NE-treated NRCMs with *siLin28a*, and subsequently transduced these cells with Lenti-*Pck2*. Remarkably, we found that *Pck2* overexpression was sufficient to induce hypertrophic growth of the NE-treated NRCMs even in the absence of *Lin28a* function (Figure 5Q and5R), suggesting that Pck2 acted epistatically to Lin28a to regulate NRCMs hypertrophy. To directly determine the epistatic relationship of Lin28a and Pck2, we knocked down *Pck2* in Lenti-*Lin28a* transduced NRCMs, and found that knockdown of *Pck2* suppressed Lin28a-induced NRCMs hypertrophy (Figure 5S and5T). The above data thus indicate that *Pck2* functions to mediate, at least in part, the effect of Lin28a in cardiac hypertrophic growth.

Lin28a/Pck2 Promotes Cardiac Glycolysis and Anabolic Synthesis

Because hypertrophic heart features an increased reliance on glucose metabolism, we monitored the glycolytic capacity of NRCMs by measuring the extracellular acidification rate (ECAR) of the surrounding media (Figure 6A). As expected, NE treatment resulted in a significant increase in the glycolytic capacity of NRCMs compared to vehicle treatment (Figure 6B). Significantly enhanced NRCMs glycolytic capacity was also observed in *Lin28a* or *Pck2* overexpressing NRCMs compared to the control cells (Figure 6B). This enhanced glycolytic metabolism was accompanied by compromised capacity to utilize palmitate as energy source (Supplemental Figure 9A–9D), consistent with the data that cardiac deletion of *Lin28a* may improve the oxidative metabolism after TAC operation (Figure 4B–4E and Supplemental Figure 6). Giving the ability of Lin28 and Pck2 to promote glycolysis, we examined the expression of glucose transporter and genes encoding key glycolytic enzymes and found significant upregulation of glucose transporter 1(*Slc2a1*),

hexokinase 1(*Hk1*) and muscle pyruvate kinase (*Pkm*) upon *Lin28* or *Pck2* overexpression (Supplemental Figure 9E–9H). Interestingly, knockdown of *Lin28a* suppressed NE-induced enhancement of cardiac glycolysis (Figure 6C). Consistently, gene expression analysis also showed that the upregulation of the key glycolytic genes induced by NE was attenuated by knockdown of *Lin28a* or *Pck2* (Supplemental Figure 9I–9L). We also evaluated the effect of *Pck2* overexpression on glycolytic rate of the NE and si*Lin28a* treated NRCMs. ECAR measurements demonstrated that *Pck2* overexpression could partly reversed the suppression of NE-induced enhancement of NRCMs glycolysis by *Lin28a* knockdown (Figure 6D).

Next, we used stable isotope tracing of glucose to further determine the effects of *Lin28a* or *Pck2* overexpression on cardiac glycolysis. The incorporation of U-^{13}C-glucose was monitored using liquid chromatography (LC) coupled to high resolution mass spectrometry (HRMS).[33] Metabolism of U-^{13}C-glucose is depicted in Figure 6E. Glycolytic and Pck2-mediated metabolic fluxes are highlighted in blue and orange, respectively (Figure 6E–6G, and Supplemental Table 3). Consistent with the role of Pck2 in catalyzing the conversion of oxaloacetate (OAA) from TCA cycle to phosphoenolpyruvate (PEP), NE treatment and *Lin28a* or *Pck2* overexpression resulted in a significant increase in the production of ^{13}C-labeled OAA-derived PEP (Figure 6F and6H). Likewise, *Lin28a* or *Pck2* overexpression significantly increased the relative abundance of glycolytic metabolites, including glucose 6-phosphate (G6P) and 3-phosphoglycerate (3PG) (Figure 6I and6J). Interestingly, this increase in glycolytic metabolites abundance was attributable to enhanced production of both U-^{13}C-Glucose-derived and ^{13}C-labeled OAA-derived glycolytic metabolites (Figure 6F–6K).

Pck2-mediated synthesis of PEP could be channeled to biosynthesis required for cell growth,[34, 35] we determined the effect of *Lin28a*/*Pck2* overexpression on the synthesis of anabolic metabolites. LC/HRMS analysis demonstrated that *Lin28a* or *Pck2 overexpression led to significantly increased relative abundance of Pck2-mediated synthesis of OAA-derived* ribose 5-phosphate (R5P) (Figure 6L). This enhanced production of R5P in turn contributed to an increased nucleotide synthesis as indicated by the upregulated levels of nucleotides, such as adenosine triphosphate (ATP) and uridine triphosphate (UTP) (Supplemental Figure 10A–10C). Cardiomyocyte hypertrophic growth also requires synthesis of lipids for the generation of biological membranes.[36] The production of OAA-derived glycerol 3-phosphate (G3P), an important starting material for *de novo* synthesis of glycerophospholipids, was remarkably enhanced upon *Lin28a* or *Pck2* overexpression (Figure 6M). Serine is the essential precursor for nucleotides, proteins and lipids during cell growth.[37] We addressed whether overexpression of *Lin28a* or *Pck2* could promote the production of OAA-derived serine. Among all the ^{13}C-labeled serine, the m+2 fractions directly generated from OAA mediated by Pck2 increased by 1.75 ± 0.14 and 1.34 ± 0.05 folds (Figure 6N), respectively, in *Lin28a* or *Pck2* overexpressing cardiomyocytes. In addition to the increased production of OAA-derived anabolic metabolites, the levels of the fully labeled anabolic metabolites were also significantly elevated (Figure 6E, and 6H–6N). It is worth noting that the increase in glycolytic and anabolic metabolites in NE-treated, *Lin28a* or *Pck2* overexpressing cardiomyocytes was not at the expense of TCA cycle intermediates, as the levels of the major TCA metabolites such as α- ketoglutarate, succinate, and fumarate remained comparable to, if not higher than, those in the control

cardiomyocytes (Figure 6O). While the enhanced production of anabolic metabolites may be explained by the increased abundance of glycolytic intermediates, which serve as the precursors for biosynthesis, we found that *Lin28*/*Pck2* overexpression also upregulated the expression of genes encoding the key metabolic enzymes in the pentose phosphate pathway, serine biosynthesis, and one-carbon metabolic pathways, including glucose-6-phosphate dehydrogenase (*G6pd*), phosphogluconate dehydrogenase (*Pgd*), phosphoglycerate dehydrogenase (*Phgdh*), phosphoserine aminotransferase 1 (*Psat1*), methylenetetrahydrofolate dehydrogenase 1 like (*Mthfd1l*) and methylenetetrahydrofolate dehydrogenase 2 (*Mthfd2*) (Supplemental Figure 10D–10I). This increase in the expression of one carbon metabolic genes *Mthfd1l* and *Mthfd2* suggests that the serine that enters one carbon metabolism may be further utilized within the activated folate cycle to support cell growth.[38] Conversely, knockdown of *Lin28a* or *Pck2* and cardiac ablation of *Lin28a* attenuated the upregulation of these key biosynthetic genes induced by NE and TAC, respectively (Supplemental Figure 10J–10P). These observations are consistent with GSEA and IPA analysis of the RNA-sequencing data showing that the biosynthetic pathways are enriched in the differentially expressed genes between TAC-operated $Lin28a^{Cko}$ and control hearts (Supplemental Figure 6 and Supplemental Figure 10Q). Our data thus implicate Lin28a/Pck2-dependent enhancement of biosynthesis and glycolysis as a mechanism for cardiomyocyte hypertrophic growth.

DISCUSSION

Hypertrophic response to pathological stimuli is a complex biological process that involves transcriptional, posttranscriptional, and epigenetic regulation of the cardiac genome. Despite substantial progress in our understanding of the molecular and physiological basis of this detrimental process, much remains to be learned. Here, we report that Lin28a plays a pivotal role in pathological cardiac hypertrophy. Cardiac-specific deletion of *Lin28a* blunted pressure overload-induced cardiac hypertrophy and suppressed cardiac fibrosis. More importantly, *Lin28a* conditional knockout mice showed preserved cardiac function and improved long-term survival. Likewise, in an *in vitro* model of cardiac hypertrophy, knockdown of *Lin28a* attenuated NE-induced hypertrophy, while overexpressing *Lin28a* alone was sufficient to stimulate cardiomyocyte hypertrophic growth. Further study indicated that the role of *Lin28a* in cardiac hypertrophic growth was mediated at least in part by *Pck2*, which in turn promoted cardiac glycolysis and biosynthesis during cardiac hypertrophy. While knockdown of *Pck2* suppressed Lin28a-induced cardiomyocyte hypertrophic growth, overexpressing *Pck2* reversed the attenuation of NE-induced hypertrophy by loss of *Lin28a* function. Together, our study indicated that Lin28a acts as a crucial regulator of pathological cardiac hypertrophy via regulating cardiomyocyte glycolysis and biosynthesis.

Lin28 was initially characterized in *C. elegans* for its role in controlling developmental timing. The vertebrate genome contains two Lin28 paralogues, Lin28a and Lin28b. Over the last three decades, the Lin28 paralogues have been primarily implicated in promoting pluripotency and carcinogenesis,[12] yet its roles in terminally differentiated organs such as heart, especially under stress conditions, remains largely unknown. In this study, we found that the expression of *Lin28a*, but not *Lin28b*, was stimulated by pathological hypertrophic

stimuli. This observation is reminiscent of the differential stabilization of Lin28a through MAPK-dependent posttranscriptional mechanism.[39] Though it is not clear whether Lin28a could also be stabilized at the protein level during pathological cardiac hypertrophy, our finding highlights a previously unappreciated differential regulation of *Lin28* paralogous at the transcriptional level. The *Lin28* paralogues are thought to have arisen by gene duplication, yet their distinct and overlapping functions still await to be fully characterized. In light of the recent reports that Lin28a is primarily localized in the cytoplasm while Lin28b is predominantly found in the nucleus,[40] it is conceivable the relative distinct subcellular localization might contribute to the distinct roles the two Lin28 proteins play in regulating diverse cellular processes.

During pathological hypertrophy, the early response genes, such as *c-Fos, c-Jun*, and *c-Myc*, are generally induced within 30 minutes after pathological stimulation.[41] Our observation that the induction of *Lin28a* slightly lagged behind that of the early response genes suggest that *Lin28a* could be directly activated by these factors. Indeed, previous studies indicated that c-Myc bind to the promoter of *Lin28a* and activate its transcription in cancer cells.[18, 19] It will be interesting to determine if *Lin28a* is a direct target of c-Myc in cardiac tissue during pathological hypertrophy. Pathological hypertrophic stimuli induce extensive and dynamic changes in cardiac transcriptome at both transcriptional and posttranscriptional levels. miRNA-mediated RNA decay has been shown to be a critical component of the posttranscriptional mechanisms to fine-tune the cardiac transcriptome, yet several lines of evidence imply that increased mRNA stability may also contribute to the dynamic regulation of cardiac transcriptome during hypertrophic growth.[42, 43] Lin28a directly binds to diverse mRNAs[31] and enhances their stability and translation efficiency.[17, 44] This regulatory mechanism of gene expression could poise the cells to readily adapt to external challenges. Consistently, our data showed that cardiac conditional knockout of *Lin28a* largely mitigated the alterations in cardiac transcriptome induced by pressure overload. Thus, Lin28a-mediated transcript stabilization represents another type of posttranscriptional regulatory mechanism during pathological hypertrophy.

Metabolic reprogramming is one of the major hallmarks of cardiac hypertrophy, as the hypertrophic heart relies more on glucose metabolism than fatty acid oxidation.[6] It is interesting to note that most of genes affected by the loss of *Lin28a* at the early phase of cardiac hypertrophy are enriched in metabolism and related pathways. Additionally, glycolytic capacity assay and metabolic flux analysis using ^{13}C-glucose further demonstrated that Lin28a functioned to increase glycolysis and anabolic pathways at the expense of compromised oxidative capacity in the hypertrophied cardiomyocytes. Our findings are thus not only consistent with previous findings that Lin28a functions as primal regulator of glucose metabolism in diabetes,[14] wound healing,[15] oncogenesis,[16] and pluripotency,[12] but also highlight its distinct role in the adult heart under stress conditions. More importantly, we identified *Pck2* as a critical direct target of Lin28a in cardiomyocytes. Manipulation of *Pck2* expression recapitulated the phenotypes of manipulating *Lin28a* knockdown or overexpression, demonstrating the crucial role of Lin28a/Pck2 axis in metabolic reprogramming during cardiac hypertrophy. Cardiomyocytes subjected to hypertrophic stimuli exhibit increased demands for protein, lipid, and nucleotide synthesis to fulfill the requirement for cell growth.[6] Pck2 diverts carbon substrates from the tricarboxylic

acid (TCA) cycle to glycolysis flux, thereby enhancing anabolic synthesis from glycolytic intermediates to support cardiomyocyte growth. Recent studies have shown that PEPCK/Pck2 may function as common regulators to promote glucose or glutamine utilization towards biosynthetic pathways to promote proliferation or cell growth.[34, 35] On the other hand, Pck2-mediated one-carbon signals may directly impact histone modification to influence gene expression.[45] Our study provides strong evidence that *Lin28a* is major regulator of pathological cardiac hypertrophy, which directly bound *Pck2* mRNA to facilitate the metabolic re-patterning in response to cardiac stress. These results are consistent with previous findings that metabolic shift precedes ventricular hypertrophic growth,[46–48] and support the idea that metabolic re-patterning during early stage of cardiac hypertrophy could be instrumental in cardiac structural remodeling. Thus, the identification of metabolic regulators, such as Lin28a/Pck2, may provide potential therapeutic options to those who suffer from pathological hypertrophy and heart failure.

Supplementary Material

Refer to Web version on PubMed Central for supplementary material.

Acknowledgements

We thank Dr. Daley for generously sharing the *Lin28a*$^{fl/fl}$ mice line. We thank UNC Rodent Advanced Surgical Models Core, UNC High-Throughput Sequencing Facility, UNC Histology Research Core Facility, and UNC Microscopy Services Laboratory for technical support. We also thank Dr. Jing Zhang in Dr. Qing Zhang lab and Dr. Aiwen Jin in Dr. Yanping Zhang lab in the UNC Lineberger Comprehensive Cancer Center for help running the experiments utilizing the Seahorse Bioscience XF24 analyzer. We thank members of the Qian laboratory and the Liu laboratory for helpful discussions and critical reviews of the manuscript.

Sources of Funding

This study was supported by American Heart Association (AHA) 13SDG17060010, Ellison Medical Foundation (EMF) AG-NS-1064–13, and NIH/National Heart, Lung, and Blood Institute (NHLBI) R01HL128331 to L.Q., NIH/National Heart, Lung, and Blood Institute (NHLBI) R00 HL109079, R56HL133081, and American Heart Association (AHA) 15GRNT25530005 to J.L.

REFERENCES

1. Frey N, Katus HA, Olson EN and Hill JA. Hypertrophy of the heart: a new therapeutic target? Circulation. 2004;109:1580–1589. [PubMed: 15066961]
2. Hill JA and Olson EN. Cardiac plasticity. N Engl J Med. 2008;358:1370–1380. [PubMed: 18367740]
3. Xie M, Burchfield JS and Hill JA. Pathological ventricular remodeling: therapies: part 2 of 2. Circulation. 2013;128:1021–1030. [PubMed: 23979628]
4. Whelton PK, Carey RM, Aronow WS, Casey DE,, Jr., Collins KJ, Dennison Himmelfarb C, DePalma SM, Gidding S, Jamerson KA, Jones DW, MacLaughlin EJ, Muntner P, Ovbiagele B, Smith SC, Jr., Spencer CC, Stafford RS, Taler SJ, Thomas RJ, Williams KA, Sr., Williamson JD and Wright JT, Jr. 2017 ACC/AHA/AAPA/ABC/ACPM/AGS/APhA/ASH/ASPC/NMA/PCNA Guideline for the Prevention, Detection, Evaluation, and Management of High Blood Pressure in Adults: A Report of the American College of Cardiology/American Heart Association Task Force on Clinical Practice Guidelines. Circulation. 2018;138(17):e484–e594. [PubMed: 30354654]
5. Katholi RE and Couri DM. Left ventricular hypertrophy: major risk factor in patients with hypertension: update and practical clinical applications. Int J Hypertens. 2011;2011:495349. [PubMed: 21755036]

6. Kolwicz SC, Jr. and Tian R. Glucose metabolism and cardiac hypertrophy. Cardiovasc Res. 2011;90:194–201. [PubMed: 21502371]
7. Friddle CJ, Koga T, Rubin EM and Bristow J. Expression profiling reveals distinct sets of genes altered during induction and regression of cardiac hypertrophy. Proc Natl Acad Sci U S A. 2000;97:6745–6750. [PubMed: 10829065]
8. Heineke J and Molkentin JD. Regulation of cardiac hypertrophy by intracellular signalling pathways. Nat Rev Mol Cell Biol. 2006;7:589–600. [PubMed: 16936699]
9. Brinegar AE and Cooper TA. Roles for RNA-binding proteins in development and disease. Brain Res. 2016;1647:1–8. [PubMed: 26972534]
10. Gerstberger S, Hafner M and Tuschl T. A census of human RNA-binding proteins. Nat Rev Genet. 2014;15:829–845. [PubMed: 25365966]
11. Fu XD and Ares M, Jr.Context-dependent control of alternative splicing by RNA-binding proteins. Nat Rev Genet. 2014;15:689–6701. [PubMed: 25112293]
12. Viswanathan SR and Daley GQ. Lin28: A microRNA regulator with a macro role. Cell. 2010;140:445–449. [PubMed: 20178735]
13. Tsialikas J and Romer-Seibert J. LIN28: roles and regulation in development and beyond. Development. 2015;142:2397–2404. [PubMed: 26199409]
14. Zhu H, Shyh-Chang N, Segre AV, Shinoda G, Shah SP, Einhorn WS, Takeuchi A, Engreitz JM, Hagan JP, Kharas MG, Urbach A, Thornton JE, Triboulet R, Gregory RI, Consortium D, Investigators M, Altshuler D and Daley GQ. The Lin28/let-7 axis regulates glucose metabolism. Cell. 2011;147:81–94. [PubMed: 21962509]
15. Shyh-Chang N, Zhu H, Yvanka de Soysa T, Shinoda G, Seligson MT, Tsanov KM, Nguyen L, Asara JM, Cantley LC and Daley GQ. Lin28 enhances tissue repair by reprogramming cellular metabolism. Cell. 2013;155:778–792. [PubMed: 24209617]
16. Ma X, Li C, Sun L, Huang D, Li T, He X, Wu G, Yang Z, Zhong X, Song L, Gao P and Zhang H. Lin28/let-7 axis regulates aerobic glycolysis and cancer progression via PDK1. Nat Commun. 2014;5:5212. [PubMed: 25301052]
17. Balzer E and Moss EG. Localization of the developmental timing regulator Lin28 to mRNP complexes, P-bodies and stress granules. RNA Biol. 2007;4:16–25. [PubMed: 17617744]
18. Chang TC, Zeitels LR, Hwang HW, Chivukula RR, Wentzel EA, Dews M, Jung J, Gao P, Dang CV, Beer MA, Thomas-Tikhonenko A and Mendell JT. Lin-28B transactivation is necessary for Myc-mediated let-7 repression and proliferation. Proc Natl Acad Sci U S A. 2009;106:3384–3389. [PubMed: 19211792]
19. Dangi-Garimella S, Yun J, Eves EM, Newman M, Erkeland SJ, Hammond SM, Minn AJ and Rosner MR. Raf kinase inhibitory protein suppresses a metastasis signalling cascade involving LIN28 and let-7. EMBO J. 2009;28:347–358. [PubMed: 19153603]
20. Weber KT and Brilla CG. Pathological hypertrophy and cardiac interstitium. Fibrosis and renin-angiotensin-aldosterone system. Circulation. 1991;83:1849–1865. [PubMed: 1828192]
21. Kong P, Christia P and Frangogiannis NG. The pathogenesis of cardiac fibrosis. Cell Mol Life Sci. 2014;71:549–574. [PubMed: 23649149]
22. Dobaczewski M, Chen W and Frangogiannis NG. Transforming growth factor (TGF)-beta signaling in cardiac remodeling. J Mol Cell Cardiol. 2011;51:600–606. [PubMed: 21059352]
23. Khalil H, Kanisicak O, Prasad V, Correll RN, Fu X, Schips T, Vagnozzi RJ, Liu R, Huynh T, Lee SJ, Karch J and Molkentin JD. Fibroblast-specific TGF-beta-Smad2/3 signaling underlies cardiac fibrosis. J Clin Invest. 2017;127:3770–3783. [PubMed: 28891814]
24. Daniels A, van Bilsen M, Goldschmeding R, van der Vusse GJ and van Nieuwenhoven FA. Connective tissue growth factor and cardiac fibrosis. Acta Physiol (Oxf). 2009;195:321–338. [PubMed: 19040711]
25. Accornero F, van Berlo JH, Correll RN, Elrod JW, Sargent MA, York A, Rabinowitz JE, Leask A and Molkentin JD. Genetic Analysis of Connective Tissue Growth Factor as an Effector of Transforming Growth Factor beta Signaling and Cardiac Remodeling. Mol Cell Biol. 2015;35:2154–2164. [PubMed: 25870108]
26. Viswanathan SR, Daley GQ and Gregory RI. Selective blockade of microRNA processing by Lin28. Science. 2008;320:97–100. [PubMed: 18292307]

27. Heo I, Joo C, Cho J, Ha M, Han J and Kim VN. Lin28 mediates the terminal uridylation of let-7 precursor MicroRNA. Mol Cell. 2008;32:276–284. [PubMed: 18951094]
28. Yang Y, Ago T, Zhai P, Abdellatif M and Sadoshima J. Thioredoxin 1 negatively regulates angiotensin II-induced cardiac hypertrophy through upregulation of miR-98/let-7. Circ Res. 2011;108:305–313. [PubMed: 21183740]
29. Polesskaya A, Cuvellier S, Naguibneva I, Duquet A, Moss EG and Harel-Bellan A. Lin-28 binds IGF-2 mRNA and participates in skeletal myogenesis by increasing translation efficiency. Genes Dev. 2007;21:1125–1138. [PubMed: 17473174]
30. Balzer E, Heine C, Jiang Q, Lee VM and Moss EG. LIN28 alters cell fate succession and acts independently of the let-7 microRNA during neurogliogenesis in vitro. Development. 2010;137:891–900. [PubMed: 20179095]
31. Hafner M, Max KE, Bandaru P, Morozov P, Gerstberger S, Brown M, Molina H and Tuschl T. Identification of mRNAs bound and regulated by human LIN28 proteins and molecular requirements for RNA recognition. RNA. 2013;19:613–626. [PubMed: 23481595]
32. Cho J, Chang H, Kwon SC, Kim B, Kim Y, Choe J, Ha M, Kim YK and Kim VN. LIN28A is a suppressor of ER-associated translation in embryonic stem cells. Cell. 2012;151:765–777. [PubMed: 23102813]
33. Liu X, Romero IL, Litchfield LM, Lengyel E and Locasale JW. Metformin Targets Central Carbon Metabolism and Reveals Mitochondrial Requirements in Human Cancers. Cell Metab. 2016;24:728–739. [PubMed: 27746051]
34. Brown DM, Williams H, Ryan KJ, Wilson TL, Daniel ZC, Mareko MH, Emes RD, Harris DW, Jones S, Wattis JA, Dryden IL, Hodgman TC, Brameld JM and Parr T. Mitochondrial phosphoenolpyruvate carboxykinase (PEPCK-M) and serine biosynthetic pathway genes are co-ordinately increased during anabolic agent-induced skeletal muscle growth. Sci Rep. 2016;6:28693. [PubMed: 27350173]
35. Montal ED, Dewi R, Bhalla K, Ou L, Hwang BJ, Ropell AE, Gordon C, Liu WJ, DeBerardinis RJ, Sudderth J, Twaddel W, Boros LG, Shroyer KR, Duraisamy S, Drapkin R, Powers RS, Rohde JM, Boxer MB, Wong KK and Girnun GD. PEPCK Coordinates the Regulation of Central Carbon Metabolism to Promote Cancer Cell Growth. Mol Cell. 2015;60:571–583. [PubMed: 26481663]
36. Ferrans VJ, Jones M, Maron BJ and Roberts WC. The nuclear membranes in hypertrophied human cardiac muscle cells. Am J Pathol. 1975;78:427–460. [PubMed: 164122]
37. Ye J, Mancuso A, Tong X, Ward PS, Fan J, Rabinowitz JD and Thompson CB. Pyruvate kinase M2 promotes de novo serine synthesis to sustain mTORC1 activity and cell proliferation. Proc Natl Acad Sci U S A. 2012;109:6904–6909. [PubMed: 22509023]
38. Ducker GS and Rabinowitz JD. One-Carbon Metabolism in Health and Disease. Cell Metab. 2017;25:27–42. [PubMed: 27641100]
39. Tsanov KM, Pearson DS, Wu Z, Han A, Triboulet R, Seligson MT, Powers JT, Osborne JK, Kane S, Gygi SP, Gregory RI and Daley GQ. LIN28 phosphorylation by MAPK/ERK couples signalling to the post-transcriptional control of pluripotency. Nat Cell Biol. 2017;19:60–67. [PubMed: 27992407]
40. Piskounova E, Polytarchou C, Thornton JE, LaPierre RJ, Pothoulakis C, Hagan JP, Iliopoulos D and Gregory RI. Lin28A and Lin28B inhibit let-7 microRNA biogenesis by distinct mechanisms. Cell. 2011;147:1066–1079. [PubMed: 22118463]
41. Izumo S, Nadal-Ginard B and Mahdavi V. Protooncogene induction and reprogramming of cardiac gene expression produced by pressure overload. Proc Natl Acad Sci U S A. 1988;85:339–343. [PubMed: 2963328]
42. Park JY, Li W, Zheng D, Zhai P, Zhao Y, Matsuda T, Vatner SF, Sadoshima J and Tian B. Comparative analysis of mRNA isoform expression in cardiac hypertrophy and development reveals multiple post-transcriptional regulatory modules. PLoS One. 2011;6:e22391. [PubMed: 21799842]
43. Fernandez-Ruiz I. Growth and development: Poly(A) tail-based regulation of cardiac hypertrophy. Nat Rev Cardiol. 2017;14:504.
44. Buchan JR and Parker R. Eukaryotic stress granules: the ins and outs of translation. Mol Cell. 2009;36:932–941. [PubMed: 20064460]

45. Zhang J, Ratanasirintrawoot S, Chandrasekaran S, Wu Z, Ficarro SB, Yu C, Ross CA, Cacchiarelli D, Xia Q, Seligson M, Shinoda G, Xie W, Cahan P, Wang L, Ng SC, Tintara S, Trapnell C, Onder T, Loh YH, Mikkelsen T, Sliz P, Teitell MA, Asara JM, Marto JA, Li H, Collins JJ and Daley GQ. LIN28 Regulates Stem Cell Metabolism and Conversion to Primed Pluripotency. Cell Stem Cell. 2016;19:66–80. [PubMed: 27320042]

46. Doenst T, Pytel G, Schrepper A, Amorim P, Farber G, Shingu Y, Mohr FW and Schwarzer M. Decreased rates of substrate oxidation ex vivo predict the onset of heart failure and contractile dysfunction in rats with pressure overload. Cardiovasc Res. 2010;86:461–470. [PubMed: 20035032]

47. Zhang L, Jaswal JS, Ussher JR, Sankaralingam S, Wagg C, Zaugg M and Lopaschuk GD. Cardiac insulin-resistance and decreased mitochondrial energy production precede the development of systolic heart failure after pressure-overload hypertrophy. Circ Heart Fail. 2013;6:1039–1048. [PubMed: 23861485]

48. Czarnowska E, Bierla JB, Toczek M, Tyrankiewicz U, Pajak B, Domal-Kwiatkowska D, Ratajska A, Smolenski RT, Mende U and Chlopicki S. Narrow time window of metabolic changes associated with transition to overt heart failure in Tgaq*44 mice. Pharmacol Rep. 2016;68:707–714. [PubMed: 27126697]

Clinical Perspective

What Is New?

- The highly conserved RNA binding protein, Lin28a, plays a critical role in pathological cardiac hypertrophy.
- Lin28a directly binds to mitochondrial phosphoenolpyruvate carboxykinase 2 (*Pck2*) mRNA to increase its transcript level and enhance cardiomyocyte biosynthesis during hypertrophic growth.
- Pck2 mediates, at least partially, the role of Lin28a in cardiac hypertrophic growth and glycolytic reprogramming.

What Are the Clinical Implications?

- The identification of Lin28a as a new regulator of pathological cardiac hypertrophy adds RNA posttranscriptional regulation as a new regulatory mechanism underlying pathological cardiac hypertrophy.
- Lin28a/Pck2-mediated metabolic re-patterning during early stage of cardiac hypertrophy is instrumental in cardiac structural remodeling, providing a potential therapeutic target for pathological cardiac hypertrophy.

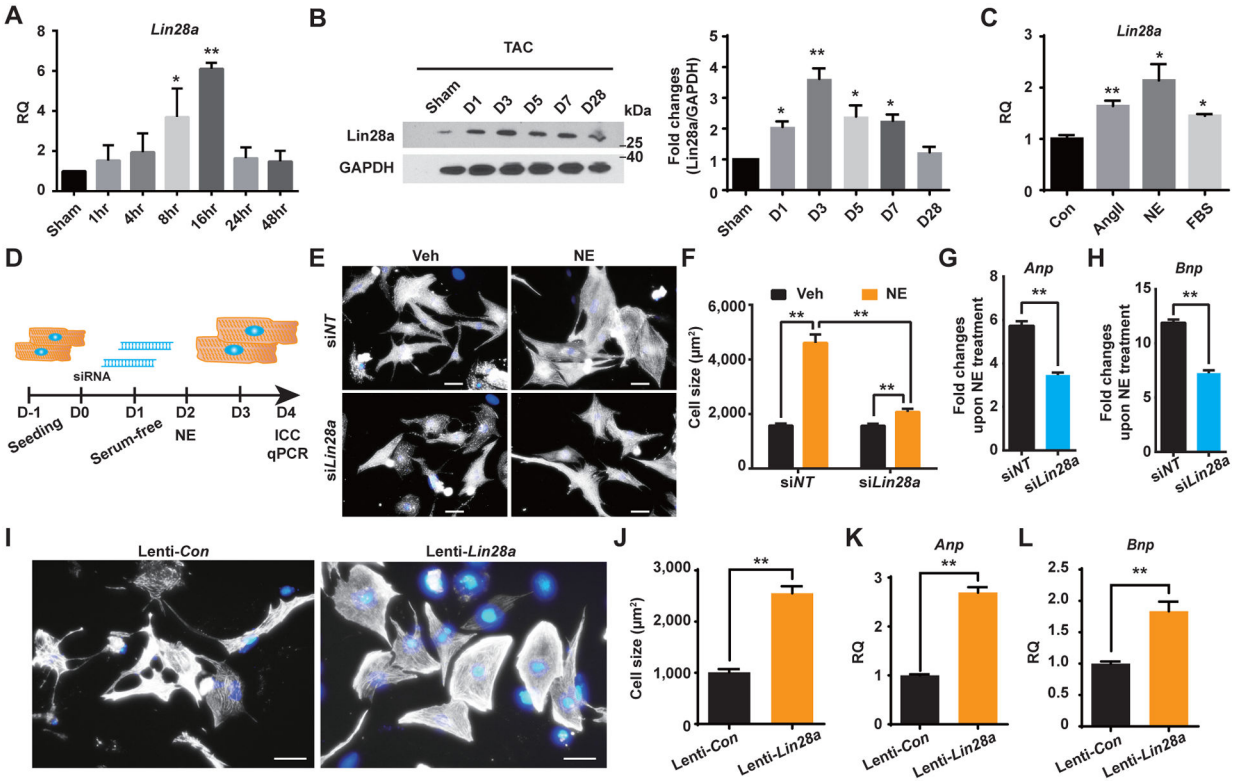

Figure 1. *Lin28a* Plays a Critical Role in NE-induced Cardiac Hypertrophy.

A, The expression level of *Lin28a* mRNA in BL6 wildtype adult mice at indicated time points after TAC surgery. **B,** Western blot analysis and quantification of Lin28a protein expression in BL6 wildtype adult mice at indicated time points following TAC. **C,** The expression level of *Lin28a* mRNA in NRCMs 12hr after angiotensin II (AngII), norepinephrine (NE), or fetal bovine serum (FBS) treatment. **D,** Schematic of siRNAs-mediated *Lin28a* knockdown in NRCMs. **E,** Representative images of α-Actinin stained cardiomyocytes treated with NE, and transfected with negative control siRNA (si*NT*) or Silencer Select validated siRNA targeting *Lin28a* (si*Lin28a*) as indicated. Nuclei were counterstained with DAPI. Scale bar, 50μm. **F,** Quantification of the cell surface area shown in panel E. **G-H,** Relative quantification (RQ) of fetal genes expression (*Anp, Bnp*) in cardiomyocytes treated with NE, and si*NT* or si*Lin28a* as indicated. **I,** Representative images of α-Actinin stained cardiomyocytes transduced with control lentiviruses (Lenti-*Con*) or lentiviruses expressing *Lin28a* (Lenti-*Lin28a*) as indicated. Nuclei are counterstained with DAPI. Scale bar, 50μm. **J,** Quantification of the cell surface area shown in panel I. **K-L,** RQ of fetal genes expression (*Anp, Bnp*) in cardiomyocytes transduced with Lenti-*Con* or Lenti-*Lin28a* as indicated.

Data are presented as mean ± SEM. **P*< 0.05; ***P*< 0.01 by *t*-test (G-H and J-L) or one-way ANOVA (A-C) or two-way ANOVA (F).

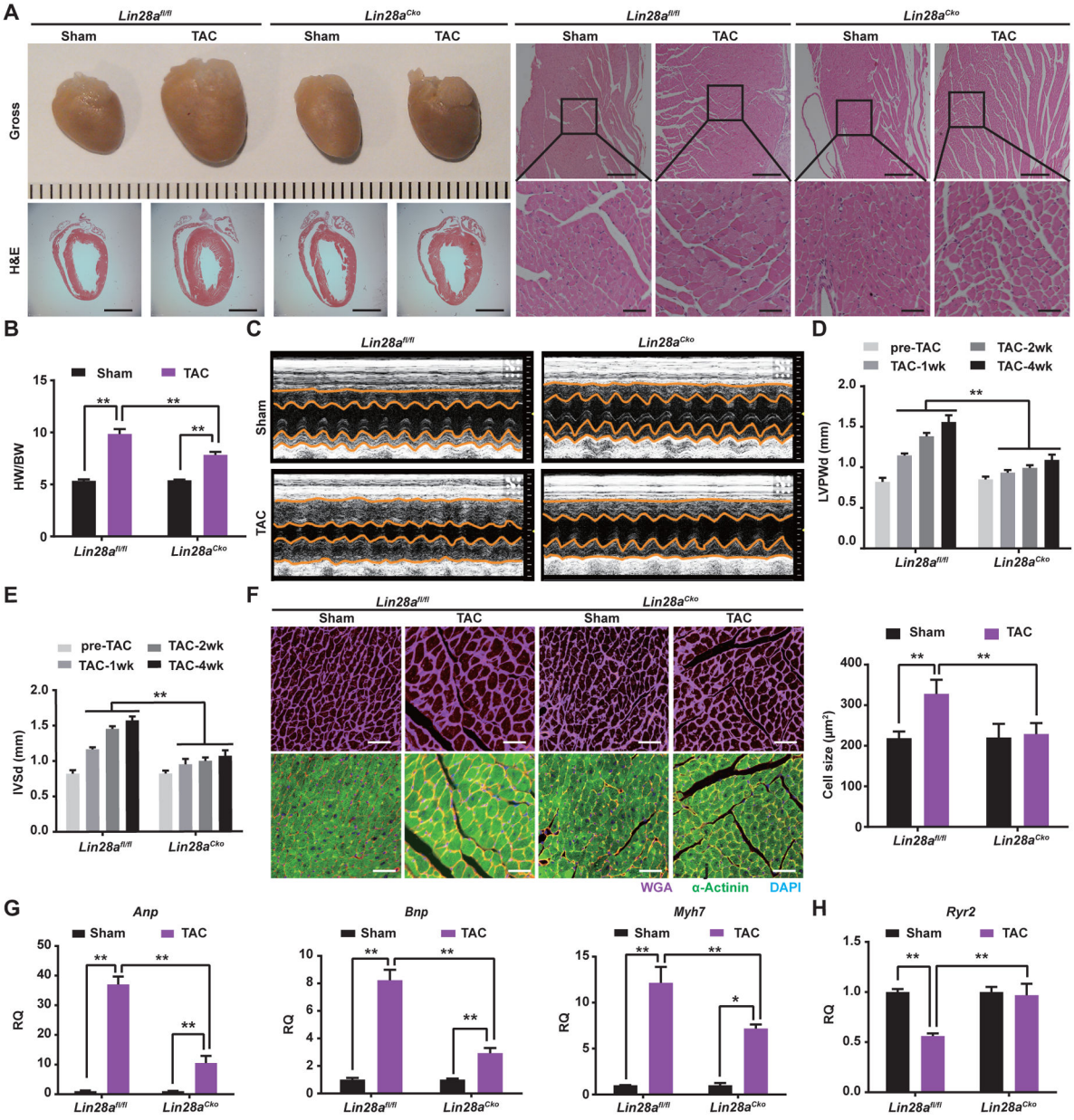

Figure 2. Cardiac Conditional Knockout of *Lin28a* Attenuates Pressure Overload-induced Cardiac Hypertrophy.

A, Representative images of gross heart morphology and H&E stained longitudinal sections of *Lin28a*^{Cko} or *Lin28a*$^{fl/fl}$ hearts at 4 weeks after TAC or sham operation. Scale bar in H&E gross image, 3mm. Scale bar in H&E section, 500μm. Scale bar in zoomed-in images, 100μm. **B,** Heart weight to body weight (HW/BW) ratio at 4 weeks after TAC or sham operations. **C,** Representative examples of M-mode echocardiography of *Lin28a*^{Cko} and *Lin28a*$^{fl/fl}$ hearts under pressure overload. **D-E,** Quantification of end-diastolic posterior wall thickness (LVPWd) (D) or end-diastolic interventricular septal wall thickness (IVSd) (E) of *Lin28a*^{Cko} and *Lin28a*$^{fl/fl}$ hearts at 1 week, 2 weeks, and 4 weeks after sham or TAC operations. **F,** Representative images of heart sections from *Lin28a*^{Cko} mice or their *Lin28a*$^{fl/fl}$ littermates at 4 weeks after sham or TAC operations. The heart sections were

immunostained with wheat germ agglutinin (WGA) in purple, α-Actinin in green and DAPI in blue. Scale bar, 100 μm. Quantification of the cross-sectional area of the cardiomyocytes shown in bar graph. **G,** RQ of the fetal gene expression (*Anp, Bnp, Myh7*) in $Lin28a^{Cko}$ and $Lin28a^{fl/fl}$ hearts at 7 days after sham or TAC operations. **H,** RQ of calcium handling gene ryanodine receptor type 2 (*Ryr2*) expression in $Lin28a^{Cko}$ and $Lin28a^{fl/fl}$ hearts at 7 days after sham or TAC operations. Data are presented as mean ± SEM. $*P<0.05$, $**P<0.01$ by two-way ANOVA (B and D-H).

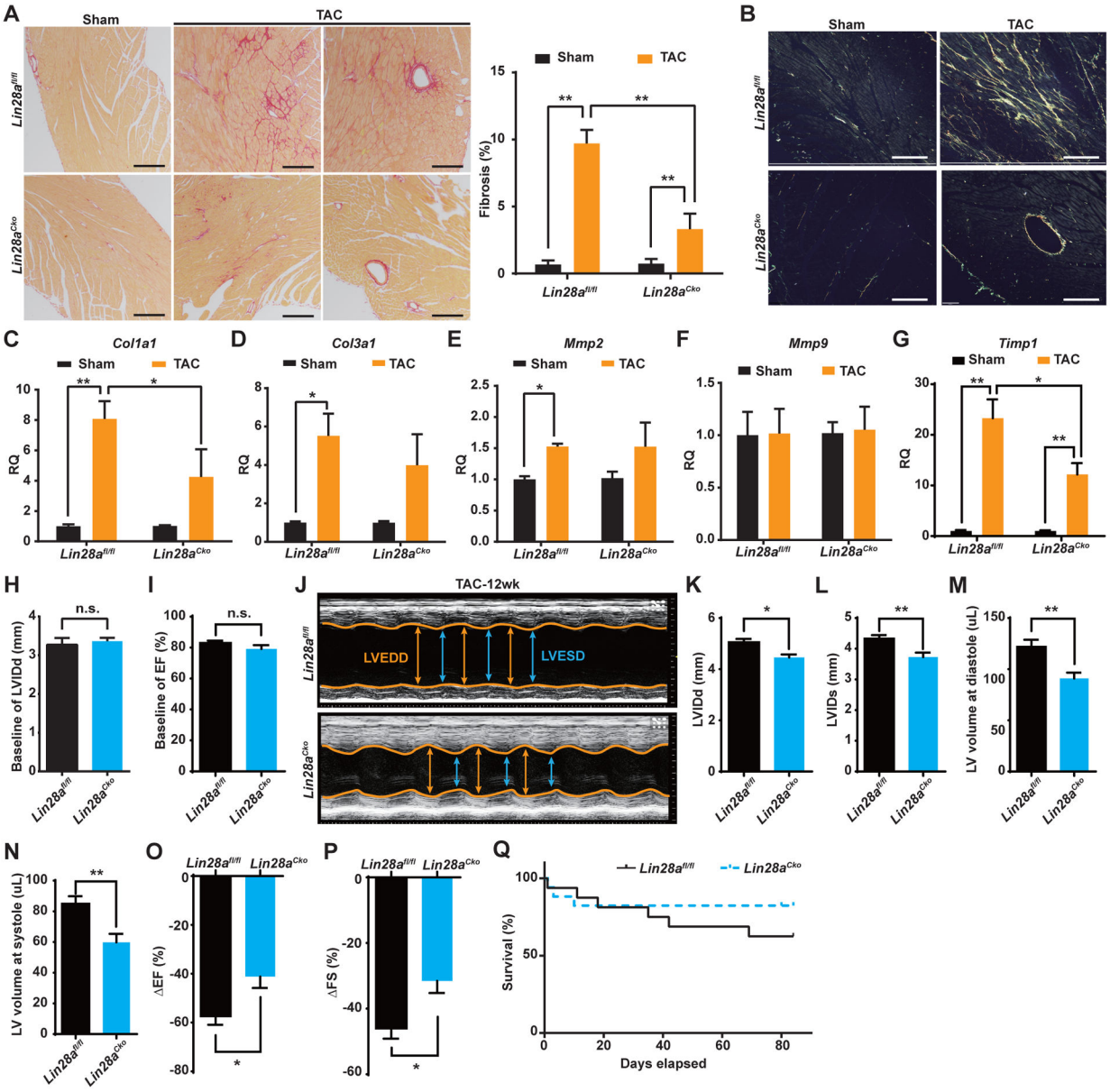

Figure 3. Pressure Overload-induced Cardiac Fibrosis and Cardiac Dysfunction Is Alleviated by Cardiac Specific Knockout of *Lin28a*.

A, Representative images of Picrosirius red stained sections from *Lin28a*^{Cko} or *Lin28a*$^{fl/fl}$ hearts at 4 weeks after sham or TAC operations. Scale bar, 500 μm. Quantification of cardiac fibrotic tissues in red is shown to the right. **B,** Representative images of Picrosirius red stained sections from *Lin28a*^{Cko} or *Lin28a*$^{fl/fl}$ hearts at 4 weeks after sham or TAC operations visualized under polarized light microscopy. Collagen type I is shown in yellow-orange. Collagen type III is shown in green. Scale bar, 500 μm. **C-G,** RQ of collagen type I α1 (*Col1a1*) (C), collagen type III α1 (*Col3a1*) (D), matrix metallopeptidase 2 (*Mmp2*) (E), matrix metallopeptidase 9 (*Mmp9*) (F) and tissue inhibitor of metalloproteinase 1 (*Timp1*) (G) expression in *Lin28a*^{Cko} and *Lin28a*$^{fl/fl}$ hearts at 7 days after sham or TAC operations. **H-I,** Quantification of left ventricle diastolic diameter (LVIDd) (H) and ejection fraction

(EF) (I) of *Lin28a*^{Cko} and *Lin28a*$^{fl/fl}$ hearts at baseline. **J,** Representative examples of M-mode echocardiography of *Lin28a*^{Cko} and *Lin28a*$^{fl/fl}$ hearts under pressure overload at 12 weeks after TAC surgery. **K-P,** Changes in LVIDd (K), left ventricle systolic diameter (LVIDs) (L), left ventricular volume at diastole (M) and systole (N), ejection fraction (EF) (O), and fraction shortening (FS) (P) in *Lin28a*^{Cko} mice and their *Lin28a*$^{fl/fl}$ littermates at 12 weeks after TAC surgery. **Q,** Survival rates of *Lin28a*^{Cko} mice and their *Lin28a*$^{fl/fl}$ littermates after sham or TAC operations. Data are presented as mean ± SEM. *P<0.05, **P<0.01; n.s., not significant by t-test (H-I and K-P), or two-way ANOVA (A and C-G).

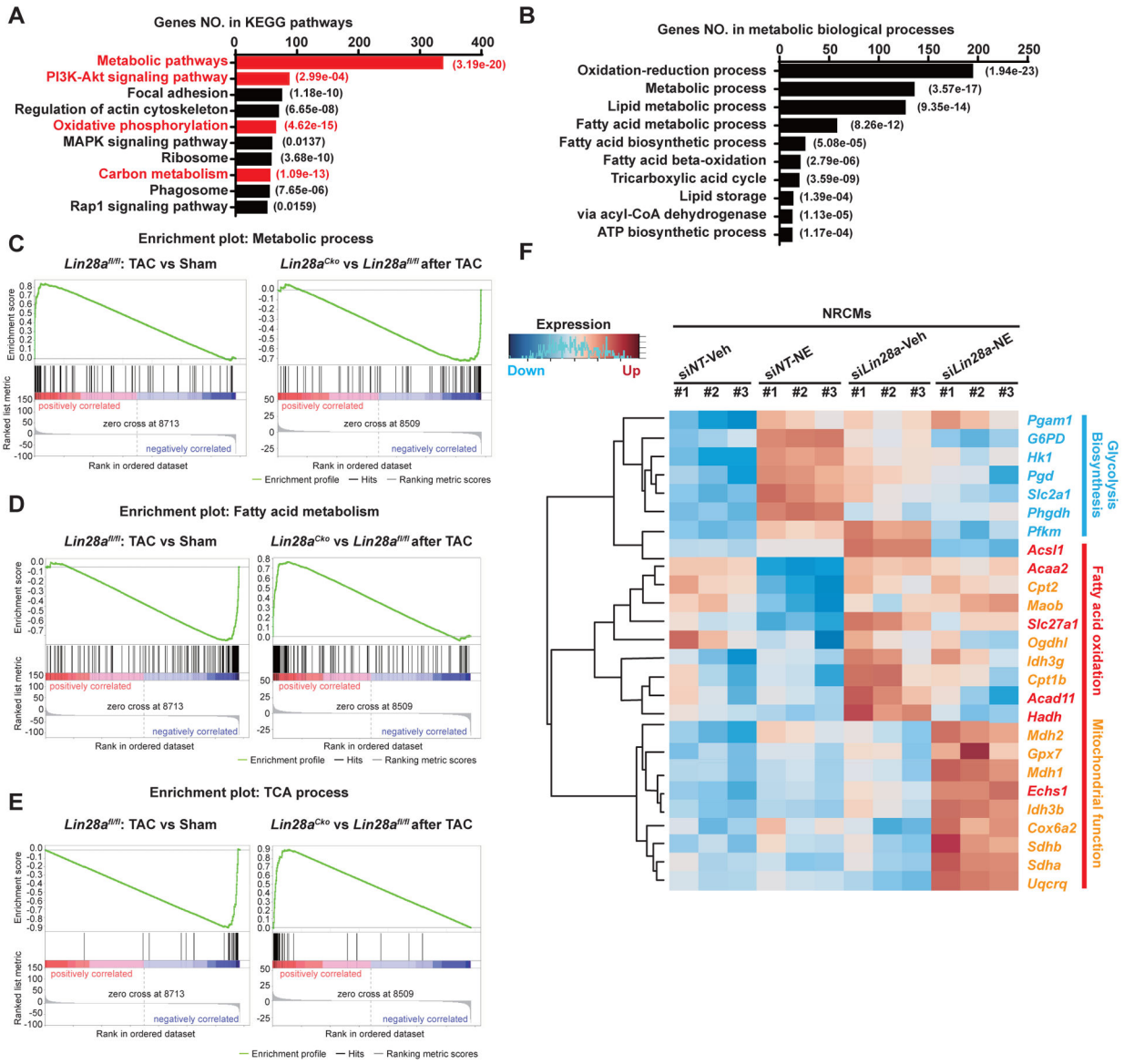

Figure 4. Loss of *Lin28a* Mitigated the Effect of TAC on Cardiac Transcriptome.

A, Functional enrichment analysis using DAVID tools. Gene Ontology (GO) annotation of the differentially expressed genes from the hypertrophied *Lin28a*^{Cko} and *Lin28a*$^{fl/fl}$ hearts. Metabolism related terms are labeled in red. **B,** GO analysis of the metabolic processes affected in the hypertrophied *Lin28a*^{Cko} and *Lin28a*$^{fl/fl}$ hearts. **C-E,** Gene set enrichment analysis (GSEA) showing the gene sets of metabolic process (C) fatty acid metabolism (D) and TCA process (E) affected by cardiac deletion of *Lin28a* in cardiac hypertrophy. **F,** Heatmaps of the relative expression of the differentially expressed genes identified in RNA-seq in cardiomyocyte transfected with negative control siRNA (si*NT*) or *Lin28a* siRNA (si*Lin28a*) under NE treatment for 48 hours *in vitro*.

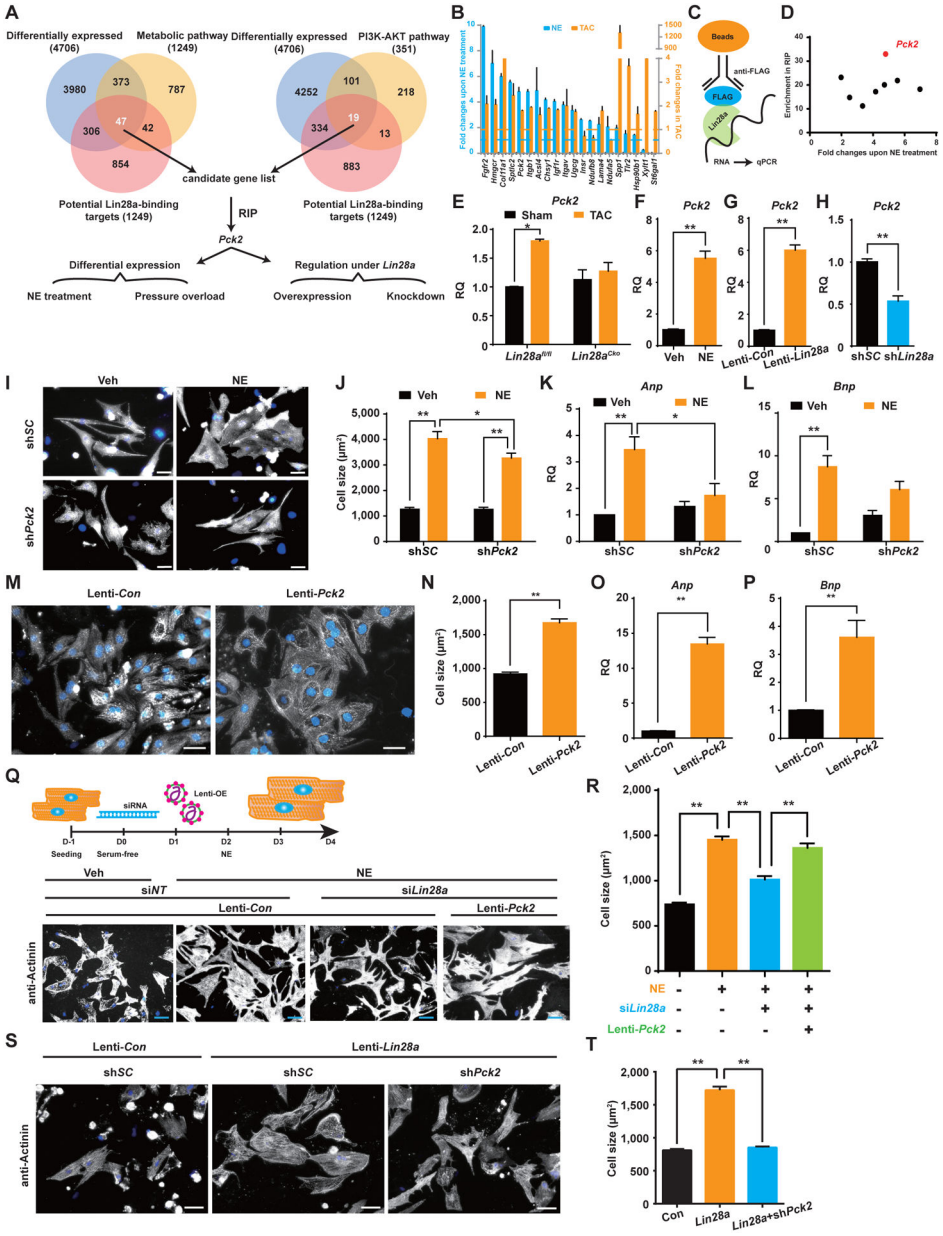

Figure 5. Pck2 Functions as a Direct Downstream Mediator of Lin28a in Cardiomyocyte Hypertrophic Growth.

A, Workflow to identify and further validate the direct targets of Lin28a involved in metabolic regulation through analysis of our RNA-seq data and published CLIP-seq data. **B,** RQ of the upregulation of the top 20 candidate target genes in cardiomyocytes in response to pressure overload *in vivo* (in orange) or NE stimulation *in vitro* (in blue). **C,** Schematic overview of RNA immunoprecipitation against FLAG-tagged Lin28a in cardiomyocytes to determine enrichment of potential Lin28a binding targets. **D,** RQ of Lin28a target genes enrichment in the Lin28a protein-RNA complex determined by RNA immunoprecipitation (RIP) assay (Y axis) and of Lin28a binding target genes upregulation in response to NE stimulation in cardiomyocytes (X axis). The dots represent the Lin28a target genes tested in 5B: *Acsl4, Chsy1, Hmgcr, Lama4, Pck2, Spp1, Sptlc2, St6gal1, Ugcg*, and *Xylt1*. **E,** RQ of

Pck2 expression in sham or TAC operated *Lin28a*^{Cko} and *Lin28a*$^{fl/fl}$ hearts. **F,** RQ of *Pck2* expression level in vehicle or NE-treated cardiomyocytes. **G,** RQ of the upregulation of *Pck2* in *Lin28a* overexpressing cardiomyocytes. **H,** RQ of *Pck2* expression in sh*SC* or sh*Lin28a* treated cardiomyocytes. **I,** Representative images of α-Actinin stained cardiomyocytes treated with NE, and sh*SC* or sh*Pck2* as indicated. Nuclei are counterstained with DAPI. Scale bar, 50 μm. **J,** Quantification of the surface area of the cells as shown in panel I. **K-L,** RQ of fetal genes expression (*Anp, Bnp*) in cardiomyocytes treated with NE, and transduced with sh*SC* or sh*Pck2* as indicated. **M,** Representative images of α-Actinin stained cardiomyocytes transduced with Lenti-*Con* or Lenti-*Pck2*. Nuclei are stained with DAPI. Scale bar, 50 μm. **N,** Quantification of the surface area of the cells as shown in panel M. For cell surface area quantification, greater than 100 cells indiscriminately selected were measured in each group. **O-P,** RQ of fetal genes expression (*Anp, Bnp*) in cardiomyocytes transduced with Lenti-*Con* or Lenti-*Pck2*. **Q,** Schematic of lentivirus-mediated *Pck2* overexpression in the *Lin28a* knockdown cardiomyocytes under NE stimulation and representative images of α-Actinin stained cardiomyocytes treated by combinations of vehicle or NE, si*NT* or si*Lin28a*, and Lenti-Con or Lenti-*Pck2* as indicated. Nuclei were counterstained with DAPI. Scale bar, 50 μm. **R,** Quantification of the surface area of the cells as shown in panel Q. **S,** Representative images of α-Actinin stained cardiomyocytes transduced with combinations of Lenti-*Con* or Lenti-*Lin28a*, sh*SC* or sh*Pck2* as indicated. Nuclei were counterstained with DAPI. Scale bar, 50 μm. **T,** Quantification of the surface area of the cells as shown in panel S. Data are presented as mean ± SEM. **P*<0.05, ***P*<0.01 by *t*-test (F-H, and N-P), or one-way ANOVA (R and T), or two-way ANOVA (E and J-L).

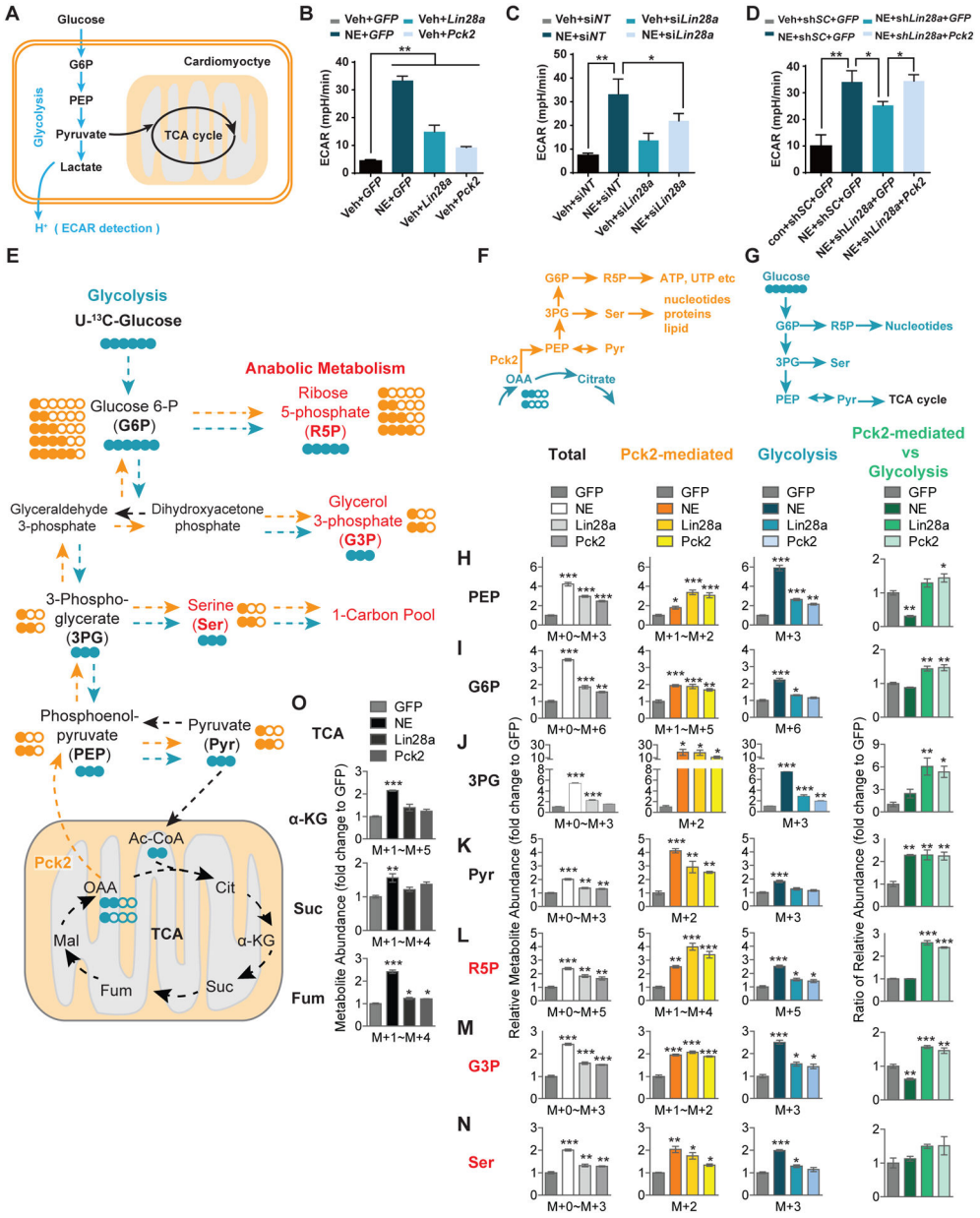

Figure 6. Lin28a/Pck2 Promotes Cardiac Glycolysis and Anabolic Synthesis.

A, Schematic of extracellular acidification rate (ECAR) measurements in cardiomyocytes. **B,** Glycolytic capacity of cardiomyocytes with control (GFP) or lentivirus mediated *Lin28a* overexpression (*Lin28a*) or *Pck2* overexpression (*Pck2*) under vehicle or NE treatment as indicated. **C,** Glycolytic capacity of cardiomyocytes treated with NE, and si*NT* or si*Lin28a* as indicated. **D,** Glycolytic capacity of cardiomyocytes treated with combinations of vehicle or NE, sh*SC* or sh*Lin28a* and GFP control or lentivirus mediated *Pck2* overexpression (*Pck2*) as indicated. **E,** Schematic of metabolism of uniformly ^{13}C labeled glucose. Glycolytic and Pck2-mediated metabolic fluxes are highlighted in blue and orange, respectively. **F,** Schematic of Pck2-mediated biosynthesis. **G,** Schematic of biosynthesis from glycolysis. **H-O,** Relative abundance of glycolytic-derived (blue) or OAA-derived

(orange) metabolic intermediates in NE-treated, *Lin28a* or *Pck2* overexpressing cardiomyocytes relative to GFP control, including PEP (H), G6P (I), 3PG (J), Pyr (K), R5P (L), G3P (M), Ser (N), and TCA intermediates α-KG, Suc, Fum (O) generated from U-^{13}C-Glucose or diverted from TCA cycle by Pck2. The sum of the indicated fractions from M+0 to M+n was labeled under the corresponding plots. Data are presented as mean ± SEM. **P*<0.05, ***P*<0.01, ****P*<0.001 by one-way ANOVA (B-D and H-O). PEP, phosphoenolpyruvate; G6P, glucose 6-phosphate; 3PG, 3-phosphoglycerate; Pyr, pyruvate; R5P, ribose 5-phosphate; G3P, glyceraldehyde 3-phosphate; Ser, serine; α-KG, α-ketoglutarate; Suc, succinate; and Fum, fumarate.